



Published in final edited form as:

Nature. 2015 May 14; 521(7551): 213–216. doi:10.1038/nature14243.

## Pathogen-Secreted Proteases Activate a Novel Plant Immune Pathway

Zhenyu Cheng<sup>1,3</sup>, Jian-Feng Li<sup>1,3,4</sup>, Yajie Niu<sup>1</sup>, Xue-Cheng Zhang<sup>1</sup>, Owen Z. Woody<sup>2</sup>, Yan Xiong<sup>1,5</sup>, Slavica Djonovi<sup>1,6</sup>, Yves Millet<sup>1,7</sup>, Jenifer Bush<sup>1</sup>, Brendan J. McConkey<sup>2</sup>, Jen Sheen<sup>1</sup>, and Frederick M. Ausubel<sup>1,\*</sup>

<sup>1</sup>Department of Genetics, Harvard Medical School and Department of Molecular Biology, Massachusetts General Hospital, Boston, MA 02114, USA

<sup>2</sup>Department of Biology, University of Waterloo, Waterloo, ON, N2L 3G1, Canada

### Abstract

Mitogen-Activated Protein Kinase (MAPK) cascades play central roles in innate immune signaling networks in plants and animals<sup>1,2</sup>. In plants, however, the molecular mechanisms of how signal perception is transduced to MAPK activation remain elusive<sup>1</sup>. We report that pathogen-secreted proteases activate a previously unknown signaling pathway in *Arabidopsis thaliana* involving the G $\alpha$ , G $\beta$  and G $\gamma$  subunits of heterotrimeric G-protein complexes, which function upstream of a MAPK cascade. In this pathway, Receptor for Activated C Kinase 1 (RACK1) functions as a novel scaffold that binds to the G $\beta$  subunit as well as to all three tiers of the MAPK cascade, thereby linking upstream G protein signaling to downstream activation of a MAPK cascade. The protease-G protein-RACK1-MAPK cascade modules identified in these studies are distinct from previously described plant immune signaling pathways such as the one elicited by bacterial flagellin, in which G proteins function downstream of or in parallel to a MAPK cascade without the involvement of the RACK1 scaffolding protein. The discovery of the novel protease-mediated immune signaling pathway described here was facilitated by the use of the broad host range, opportunistic bacterial pathogen *Pseudomonas aeruginosa*. The ability of *P. aeruginosa* to infect both plants and animals makes it an excellent model to identify novel types of immunoregulatory strategies that account for its niche adaptation to diverse host tissues and immune systems.

Reprints and permissions information is available at [www.nature.com/reprints](http://www.nature.com/reprints).

\*Correspondence and requests for materials should be addressed to F.M.A. [ausubel@molbio.mgh.harvard.edu](mailto:ausubel@molbio.mgh.harvard.edu).

<sup>3</sup>These authors contributed equally to this work

<sup>4</sup>Present address: State Key Laboratory of Biocontrol and Guangdong Key Laboratory of Plant Resources, School of Life Sciences, Sun Yat-sen University, Guangzhou, 510275, China

<sup>5</sup>Present address: Shanghai Center for Plant Stress Biology, Chinese Academy of Sciences, Shanghai, P. R. China

<sup>6</sup>Present address: Symbiota, Inc., 100 Edwin Land Blvd, Cambridge, MA 02142, USA

<sup>7</sup>Present address: Synlogic, 130 Brookline St., Cambridge, MA 02139, USA

**Author Contributions:** Z.C., J.-F.L., J.S., and F.M.A. designed experiments, Z.C., J.-F.L., Y.N., X.-C.Z., O.Z.W., Y.X., S.D., Y.M., and J.B. performed experiments, Z.C., J.-F.L., B.J.M., J.S., and F.M.A. wrote the manuscript.

### Author Information:

The authors declare no competing financial interests.

We found that culture filtrate of *P. aeruginosa* strain PA14 activates an *Arabidopsis*  $\beta$ -glucuronidase (GUS) reporter gene under the control of the pathogen-inducible *CYP71A12* promoter (*CYP71A12pro::GUS*). Whereas the well-characterized immune elicitor flg22, a synthetic peptide that corresponds to the active epitope of bacterial flagellin, induces *CYP71A12pro::GUS* in the root elongation zone<sup>3</sup>, PA14 culture filtrate activates the reporter in the cotyledons and leaves of both wild-type *Arabidopsis* Col-0 and *fls2* mutant seedlings in which the flagellin receptor is mutated (Fig. 1a).

By screening a collection of 64 *P. aeruginosa* PA14 regulatory and secretion-related mutants, we found that the induction of the *CYP71A12* promoter was dependent on the quorum-sensing gene *lasI* and on the Type II secretion apparatus-encoding genes *XcpR*, *XcpT*, *XcpW*, and *XcpZ* (Fig. 1a; Extended Data Table 1). Ion exchange chromatography fractionation (Extended Data Fig. 1a) followed by mass spectrometry (data not shown) identified the elicitor in the PA14 secretome as protease IV, a Type II-secreted, PvdS-regulated lysyl class serine protease encoded by the *P. aeruginosa* *prpL* gene (PA14\_09900). Purified His-tagged PA14 protease IV (referred to as PrpL in the Figure Legends) activated *CYP71A12pro::GUS* (Extended Data Fig. 1b), whereas culture filtrate from an in-frame deletion mutant of *prpL* (PA14/ *prpL*) did not (Fig. 1a).

Purified protease IV is a very strong elicitor of immune responses in *Arabidopsis*, comparable to flg22 in the activation of MPK3 and MPK6 (but not MPK4) (Fig. 1b), elicitation of an oxidative burst (Fig. 1c), deposition of callose in cotyledons (Fig. 1d), and protection of adult *Arabidopsis* leaves from *P. syringae* pv. *tomato* strain DC3000 infection (Fig. 1e). In contrast, trypsin, a well-characterized serine protease, failed to activate MAPK cascades or trigger an oxidative burst (Extended Data Fig. 2a, b). Global transcriptional profiling analysis (Extended Data Fig. 3a), confirmed by RT-qPCR analysis of selected defense-related genes (Extended Data Fig. 3b), showed a high degree of concordance between the genes activated or repressed by protease IV and genes previously shown to be regulated by flg22 or oligogalacturonides (OGs) in seedlings<sup>4</sup> (Pearson correlation coefficients of 0.899 and 0.864 for protease IV-treated vs. flg22 and OGs, respectively).

Importantly, protease IV variants containing alanine substitutions at the proteolytic catalytic triad site (PrpL<sup>H72A</sup>, PrpL<sup>D122A</sup>, PrpL<sup>S198A</sup>), which exhibit no detectable proteolytic activity<sup>5</sup>, were impaired for MAPK activation (Fig. 1f), defense gene induction, and oxidative burst elicitation (Extended Data Fig. 4a, d). Treatment of protease IV with the protease inhibitor TLCK (Fig. 1g, Extended Data Fig. 4b, d) or with heat (Fig. 1c, Extended Data Fig. 4c) also resulted in a loss of elicitation ability.

The closest homolog of *P. aeruginosa* protease IV in sequenced bacterial genomes is encoded by the *argC* gene of *Xanthomonas campestris*, a *bona fide* plant pathogen (Extended Data Fig. 5a). Purified His-tagged ArgC protease exhibited protease activity *in vitro* and triggered the activation of MPK3 and MPK6 that is dependent on ArgC protease activity (Fig. 1g).

We noticed that there is a high rate of naturally-occurring null mutations in the *Xanthomonas argC* gene (8 out of 22 total alleles in sequenced *Xanthomonas* genomes;

Extended Data Fig. 5b to d), suggesting that *argC* is likely under negative selection. Consistent with the sequence data, the culture filtrate of strain *X. campestris* pv. *raphani* strain 1946, from which the functional *argC* gene was cloned, activated the *CYP71A12**pro::GUS* reporter, whereas culture filtrates from two *X. campestris* pv. *campestris* strains (8004 and BP109), which contain presumptive *argC* null frame shift mutations, failed to activate (Extended Data Fig. 5e). We complemented the null *argC* mutant in strain 8004 (*Xcc* 8004) with the functional *argC* gene from strain 1946 (8004/*argC*) (Extended Data Fig. 5e). Consistent with ArgC-mediated induction of a host immune response during an infection in a mature plant, the growth of 8004/*argC* in *Brassica oleracea* (broccoli), a natural host of *X. campestris*, was reduced about 6 fold compared to the 8004/vector control (Fig. 1h). The expression of HA-tagged ArgC was readily detected in broccoli leaves infected with 8004/*argC* (Extended Data Fig. 5e), indicating that ArgC is synthesized during infection.

Next, we sought to investigate the mechanism by which protease IV activates an immune response in *Arabidopsis*. Previous studies have shown that G proteins play a role in microbe-associated molecular pattern molecules (MAMPs)-mediated responses<sup>6</sup>. In the case of protease IV, we found reduced expression of defense-related genes in *ga* or *gβ* mutants (and in a *gγ1gγ2* double mutant), reduced levels of the oxidative burst in a *ga* mutant and a *gαβ* double mutant, reduced MPK3 and MPK6 activation, and reduced protection against *P. syringae* infection in a *gαβ* double mutant (Fig. 2a to c; Extended Data Fig. 6a, b). The induction of *CYP71A12* and activation of MPK3 and MPK6 by *X. campestris* ArgC was also diminished in the G protein mutants, similar to the pattern observed for protease IV (Fig. 2a and b). In contrast to protease IV and ArgC, in the case of *flg22*, defense gene expression was only reduced in *gβ* and *gαβ* double mutants, the oxidative burst was more severely affected in a *gβ* mutant than in a *ga* mutant, protection against *P. syringae* was only modestly affected in a *gαβ* double mutant, and the activation of MAPKs was not affected in any of the G protein mutants (Fig. 2a to c, Extended Data Fig 6b). These data show that G protein signaling is required to activate downstream MAPKs in response to protease IV and ArgC, but not *flg22* (Fig. 2a), and that G proteins play different roles in canonical MAMP and protease-mediated signaling pathways.

In a search of potential signaling components that could link the heterotrimeric G-protein complex to downstream MAPK cascades, we considered the conserved scaffold protein RACK1<sup>7</sup>. The rationale was that RACK1 is homologous with Gβ<sup>7</sup>, interacts with Gβ in metazoans<sup>8</sup>, and functions in innate immune signaling in rice<sup>9</sup>. There are three RACK1 homologues in *Arabidopsis*: RACK1A, 1B, and 1C, which share 99% amino acid identity<sup>10</sup>.

We used three methods to determine whether *Arabidopsis* RACK1 proteins interact with G proteins and MAP kinases. In a bimolecular fluorescence complementation (BiFC) assay in *Nicotiana benthamiana* leaves, RACK1A, RACK1B, and RACK1C interacted with Gβ, MEKK1(K361M), MKK4, MKK5, MPK3, and MPK6, but not Gα or MPK4 (Extended Data Fig. 7a). A kinase-inactive version of MEKK1, MEKK1(K361M), was used in this experiment because the auto-activation of native MEKK1 destabilizes its interaction with RACK1 (data not shown). MEKK1, MKK4/5, and MPK3/6 are the *Arabidopsis* MAPKKK, MAPKKs, and MAPKs, respectively, that were proposed to constitute a MAP kinase-

signaling cascade in the flg22/FLS2 signaling pathway<sup>11</sup>. Similar results to those obtained with the BiFC assay in *N. benthamiana* were obtained with BiFC and split firefly luciferase complementation (SFLC) assays for RACK1A interactors in *Arabidopsis* protoplasts (Extended Data Fig. 7b, c). The interaction between RACK1 proteins and MPK3/6, but not MPK4 is consistent with the data in Fig. 1b, showing that MPK6 and MPK3, but not MPK4, are strongly activated after protease IV treatment.

In co-immunoprecipitation (Co-IP) experiments in *Arabidopsis* mesophyll protoplasts using FLAG-tagged RACK1s as the bait and HA-tagged G $\beta$  subunit as the prey, we observed binding between all three *Arabidopsis* RACK1 proteins and G $\beta$  (Fig. 3a and Extended Data Fig. 7d). In contrast to G $\beta$ , HA-tagged G $\alpha$  was not pulled down by FLAG-tagged RACK1 proteins (Fig. 3b and Extended Data Fig. 7d). In the co-IP experiments, the interaction of G $\beta$  with RACK1A was not dependent on G $\alpha$ , because the interaction was still present in the *ga $\beta$*  double mutant (Extended Data Fig. 7e). Finally, consistent with the BiFC and SFLC assays, HA-tagged MEKK1(K361M), MKK5, MPK3, and MPK6 all co-immunoprecipitated with FLAG-tagged RACK1A, whereas MPK4 did not under the same condition (Fig. 3c to f). The amounts of the MAPKK and MAPKs that were pulled down by RACK1A in the co-IP experiments clearly decreased in the presence of protease IV (Fig. 3d to f), suggesting that protease IV releases the activated MAPKs from the RACK1-MAPK cascade complex to execute their downstream cellular functions. In the case of the MAPKKK MEKK1, we also identified endogenous RACK1 proteins by mass spectrometric analysis as binding partners of MEKK1(K361M) (Extended Data Fig. 7f) in a transgenic line in which FLAG-tagged MEKK1(K361M) is expressed under the control of the 3.9-kb *MEKK1* native promoter in a *mekk1* null mutant background.

To confirm the physiological relevance of the observed interactions between RACK1 and MAPK cascade components (Fig. 3 and Extended Data Fig. 7), we tested a variety of loss-of-function MAPK mutants and knockdowns. We found that the activation of the defense-related genes *WRKY30* and *WRKY33* by protease IV was almost completely blocked in two independent *mpk3,6-es* transgenic lines in which *mpk3* is silenced with an estradiol inducible *MPK3*-RNAi construct in a null *mpk6* mutant background (Extended Data Fig. 8a). We also found that both protease IV-triggered MPK3/6 activation and *WRKY30* and *WRKY33* gene induction were disrupted in *mkk4,5-es* transgenic lines (Extended Data Fig. 8a, b), which utilize a single estradiol inducible RNAi construct to target both *MKK4* and *MKK5* mRNAs. Finally, we observed a significant decrease in protease IV-triggered induction of *WRKY30* and *WRKY33* mRNA accumulation in two *mekk1* mutants, an *mekk1* null mutant and the *mekk1* null mutant complemented with an MEKK1(K361M) construct [*mekk1/pMEKK1::MEKK1(K361M)*] (Extended Data Fig. 8c, d). As previously reported, MEKK1(K361M), which is deficient in kinase activity, rescues the severe growth defect of an *mekk1* null mutant<sup>12</sup>. In contrast to the *mkk4,5* knockdown lines, we did not consistently observe a decreased level of protease IV-triggered MPK3/6 phosphorylation in either of the *mekk1* mutants (Extended Data Fig. 8e). One explanation for the partial decrease in *WRKY* gene induction but not in MPK3/6 phosphorylation in the *mekk1* mutants is that multiple MAPKKKs<sup>13</sup> function additively to activate MPK3/6 but that the phosphorylation assay is not sensitive enough to detect a partial loss of MAPKKK activity.

Obtaining genetic evidence that RACK1 is required for protease-mediated signaling is challenging because of the functional redundancy of the three RACK1 proteins in *Arabidopsis*. T-DNA mutants corresponding to insertions in individual *rack1* genes did not show any decrease in protease IV- or flg22-activated MAPK levels (Extended Data Fig. 9a), and only moderate decreases in protease IV- but not flg22-triggered defense gene induction (Extended Data Fig. 9b). Because *rack1a rack1b rack1c* triple null mutants have a dwarf phenotype and do not set seeds<sup>14</sup>, we generated two independent transgenic lines, *amiR-rack1-es1* and *amiR-rack1-es2*, which express a previously described artificial microRNA (*amiR-RACK1-4*)<sup>15</sup> under the control of an estradiol-inducible promoter. These transgenic lines showed dramatically decreased transcript levels of all three *rack1* genes following estradiol treatment (Extended Data Fig. 9c). Following protease IV or ArgC treatment, *amiR-rack1-es1* and *amiR-rack1-es2* seedlings that had been induced with estradiol exhibited markedly decreased levels of activated MPK3 and MPK6 (Fig. 4a). Protoplasts transfected with constitutively expressed *amiR-RACK1-4* also showed reduced levels of protease IV-mediated MPK3 and MPK6 activation (Extended Data Fig. 9d, e). Similarly, knockdown of the *rack1* genes blocked protease IV or ArgC-mediated defense gene induction (Fig. 4b) and protease IV-mediated protection against *P. syringae* infection (Fig. 4c). In contrast to protease IV and ArgC, flg22-mediated activation of MAPKs or defense gene expression or protection against *P. syringae*, were not affected by knock down of the *rack1* genes (Fig. 4a to c; Extended Data Fig. 9e). These data are consistent with the conclusion that RACK1 proteins function in the protease IV and ArgC signaling pathway but not the flg22 pathway.

The RACK1 proteins studied here are the first MAPK cascade scaffolding proteins discovered for the large family of plant genes encoding MAPK cascade components. In yeast, the scaffolding protein Ste5 links a MAPK cascade to G-protein signaling in the mating pathway that is mediated by G protein coupled receptor (GPCR) stimulation by yeast pheromone<sup>16</sup>. In mammals, the scaffolding protein  $\beta$ -arrestin 2 brings MAPK cascade activity under the control of upstream GPCRs<sup>16</sup>. However, since plants do not have canonical GPCRs or orthologs of Ste5 and  $\beta$ -arrestin<sup>6,16</sup>, our data suggest that the linkage of G-proteins to MAPKs via RACK1 is mechanistically distinct from G protein signaling in metazoans and yeast.

The protease-activated signaling pathway is summarized in the model shown in Fig. 4d. It remains to be determined whether the cleavage of protein targets by protease IV directly or indirectly activates downstream responses. In the latter scenario, pathogen-secreted proteases could release host polypeptides that function as damage-associated molecular patterns (DAMPs) that are subsequently recognized by corresponding DAMP immune receptors. In either case, an evolutionary and physiological interpretation of our findings is that plants evolved a novel surveillance system to recognize and respond to pathogen-encoded proteases that disrupt host homeostasis via their proteolytic activity.

## Methods

### Bacterial strains

*P. aeruginosa* strains used in this work were wild type and mutants of UCBPP-PA14<sup>17,18</sup> and PAO ADD1976<sup>19</sup>. The latter strain carries the chromosomally incorporated gene for T7 RNA polymerase under the control of the *lac* repressor and was used for production of His-tagged PrpL and His-tagged ArgC. *Xanthomonas campestris* strains were described previously<sup>20</sup>.

A PA14/ *prpL* in-frame deletion mutant was constructed using a method described previously<sup>21</sup> that employed a sequence that contained regions immediately flanking the coding sequence of the *prpL* gene. This fragment was generated by a standard 3-step PCR protocol using Phusion DNA polymerase (New England Biolabs) and then cloned into the *Bam*HI and *Hind*III sites of pEX18Ap<sup>22</sup>, resulting in plasmid pEX18- *prpL*. pEX18- *prpL* was used to introduce the deleted region into the wild-type PA14 genome by homologous recombination. *Escherichia coli* strain SM10  $\lambda$ pir was used for triparental mating<sup>23</sup>.

For the purification of His-tagged protease IV or ArgC, the *P. aeruginosa* PA14 *prpL* gene or the *X. campestris* strain 1946 *argC* gene were cloned into the *Eco*RI and *Xho*I sites of pETP30<sup>24</sup>, creating plasmids pETP-*prpL* or pETP-*argC*, which encode 6xHis-tagged PrpL and 6xHis-tagged ArgC, respectively. The resulting plasmids were transformed into *P. aeruginosa* PAO ADD1976 by electroporation<sup>25</sup> to generate the strains ADD/pETP-*prpL* or ADD/pETP-*argC* for purification of His-tagged protease IV or His-tagged ArgC, respectively.

For *argC* complementation in *Xanthomonas*, the *X. campestris* strain 1946 *argC* gene was cloned into the *Bam*HI site of pVSP61<sup>26</sup>, creating plasmid pVSP61-*argC*. An HA-tag was incorporated at the C-terminal of the *argC* gene for the detection of the complemented protein. The resulting plasmid and empty pVSP61 vector were transformed into *X. campestris* strain 8004 by triparental conjugation<sup>23</sup>.

Antibiotics were supplemented as needed: ampicillin or carbenicillin, 50  $\mu$ g/ml for *E. coli* or 300  $\mu$ g/ml for *P. aeruginosa*; kanamycin 50  $\mu$ g/ml for *E. coli* and *Xanthomonas campestris* or 200  $\mu$ g/ml for *P. aeruginosa*; and rifampicin 100  $\mu$ g/ml.

### Construction of *Arabidopsis* transgenic lines

Construction of *amiR-rack1-es* transgenic lines and the *mekk1/pMEKK1::MEKK1(K361M)* transgenic line was carried out as follows: the *Bam*HI/*Pst*I fragment of pre-amiR-*RACK1-4*<sup>15</sup> was inserted between the estradiol-inducible promoter<sup>27</sup> and the *NOS* terminator in a modified pUC119-RCS vector<sup>28</sup>. The pre-amiR-*RACK1-4* expression cassette was then cut out by *Asc*I digestion and inserted into *Asc*I-digested binary vector pFGC19-XVE-RCS<sup>28</sup>, which expresses the XVE transcriptional activator<sup>29</sup> under the *35S* promoter, to obtain pFGC-EST-RACK1. This latter plasmid was introduced into *Agrobacterium tumefaciens* GV3101 cells by electroporation, and GV3101/ pFGC-EST-RACK1 was used to generate transgenic *Arabidopsis* plants with inducible *amiR-RACK1* expression using the floral dip technique<sup>30</sup>. To generate *mekk1/pMEKK1::MEKK1(K361M)* transgenic



*Arabidopsis*, a ~9.4 kb *MEKK1* genomic fragment was used to complement a *mekk1* null mutant (Salk\_052557). This genomic fragment contains a ~3.9 kb promoter sequence upstream of the start codon, an “AAGG” to “ATGG” mutation in exon 2 (corresponding to K361M mutation in MEKK1) to disrupt MEKK1 kinase activity, and a double FLAG-tag coding sequence upstream of the stop codon.

### Fractionation of the PA14 secretome

One liter of PA14 cells grown in M9 minimal medium (6.8 g/L Na<sub>2</sub>HPO<sub>4</sub>, 3 g/L KH<sub>2</sub>PO<sub>4</sub>, 0.5 g/L NaCl, 1 g/L NH<sub>4</sub>Cl, 2 mM MgSO<sub>4</sub>, 0.1 mM CaCl<sub>2</sub>, 10 μM FeCl<sub>3</sub>, 0.4 % glucose, 10 mg/L thiamine) was centrifuged at 20,000 × *g* at 4°C for 30 minutes and the pellet was discarded. The supernatant was filtered through a 0.22 μm low protein-binding filter (Corning). Secreted PA14 proteins in the filtrate were precipitated with ammonium sulfate (85% saturation) at 4°C overnight, followed by centrifugation at 20,000 × *g* at 4°C for 1 hour. The pellet was resuspended in 30 mL buffer A (20 mM Tris, pH 8.8), concentrated to 150 μL using Centrion Plus-70 filter (Millipore) to remove the excess ammonium sulfate, and diluted again into 10 mL buffer A. The protein sample was loaded onto a 1-mL DEAE anion exchange chromatography column (GE Healthcare) that was washed with buffer B (20 mM Tris, pH 8.8, 1 M NaCl) and equilibrated with buffer A. Proteins were separated into 1-mL fractions with a linear gradient of buffer B (0-60% within 20-column volumes). The fractionation was carried out at 4°C with a flow rate of 1 mL/minute.

### Purification of *P. aeruginosa* protease IV and *X. campestris* ArgC

Secreted proteins from ADD1976/pETP-*prpL* were precipitated as described above and resuspended in lysis buffer (50 mM NaH<sub>2</sub>PO<sub>4</sub>, 300 mM NaCl, 10 mM imidazole, pH 8.0). The sample was loaded onto a 5-mL HisTrap Affinity Column (GE Healthcare) and the 6×His tagged PA14 protease IV was purified according to the manufacturer’s instructions. The eluted protease IV was concentrated to 150 μL and immediately subjected to a Superdex 200 gel filtration column (GE Healthcare). Purified protease IV was exchanged into M9 minimal medium and filter-sterilized using a 0.22 μm low protein-binding filter (Millipore). The concentration of the purified protease IV was adjusted to 20 μM, aliquoted, and stored at –80°C before being used for plant treatments. *X. campestris* protease ArgC was purified using the same protocol.

### Protease assay

The protease activity assay of protease IV and its homolog ArgC was determined as previously described<sup>31</sup>. Protease IV and ArgC were inactivated by TLCK as previously described<sup>31</sup>.

### Plant growth

Seeds were sterilized in 20% bleach for 2 min and washed three times with sterile water. Seedlings were grown in liquid MS medium (Murashige and Skoog basal medium with vitamins from Phytotechnology Laboratories supplemented with 0.5 g/L MES hydrate and 0.5% sucrose at pH 5.7) in either 24-well assay plates (BD Falcon) (8 seeds and 0.5 mL medium/well) for MAP kinase assays, microarray and RT-qPCR analysis, callose induction

and GUS expression, or 96-well plates (Greiner Bio-One) (1 seed and 0.2 mL medium/well) for oxidative burst measurements. Plates were sealed with Micropore tape and placed on grid-like shelves over water trays on a Floralight cart in a plant growth chamber for 10 days at 21°C with 75% relative humidity under 16 hours of daylight ( $65\text{-}70 \mu\text{E}\cdot\text{m}^{-2}\cdot\text{s}^{-1}$ ). The media in 24-well plates was exchanged for fresh media on day 8, whereas the media in 96-well plates was exchanged for sterile water on day 9.

### Elicitor treatments

The synthetic peptide flg22 was synthesized by Genscript, New Jersey. Experimentally determined optimal concentrations of protease IV were: 20 nM for oxidative burst measurements, microarray and RT-qPCR analyses; 40 nM for MAP kinase activation; 100 nM for GUS expression; 500 nM for callose elicitation and the infection protection assay. For direct comparison, the same concentrations of flg22 and protease IV or ArgC were used in the same assays. Ten-day old seedlings were treated with different elicitors for the following times unless otherwise specified: 6 hours for GUS assays in reporter line *CYP71A12pro:GUS*; 10 minutes for MAP kinase activation assays; 1 hour or 6 hours for RT-qPCR analysis of selected genes; and 18 hours for callose induction.

### Transient silencing of *MAPK* or *MAPKK* genes in transgenic plants

In two independent *mpk3,6-es* transgenic lines, *MPK3* was silenced with an estradiol inducible *MPK3*-RNAi construct in a null *mpk6* mutant (Salk\_062471) background. In two *mkk4,5-es* transgenic lines, a single estradiol inducible RNAi construct was utilized to target both *MKK4* and *MKK5* mRNAs. Details concerning the construction of the *mpk3,6-es* and *mkk4,5-es* transgenic lines will be described elsewhere. The transgenic and control plants were grown in MS medium in a 24-well plate as described above for 4 days. Then the medium was changed to MS medium containing 10  $\mu\text{M}$  estradiol (Sigma, 100 mM stock in DMSO). After exposure to estradiol for 3 days, the seedlings were treated with water and 40 nM purified protease IV for 10 minutes (for MAPK assays) or 20 nM purified protease IV for 1 hour (for RT-qPCR assays).

### Transient silencing of *rack1* genes in protoplasts and transgenic plants

Mesophyll protoplasts isolated from leaves of 4-week old *Arabidopsis* plants ( $4\times 10^4$  cells in 200  $\mu\text{L}$ ) were transfected with 40  $\mu\text{g}$  (20  $\mu\text{L}$ ) of amiR-*RACK1*-4 construct or empty amiRNA expression vector<sup>15</sup> as a control. After 24 hours of expression, 100 nM flg22 or 100 nM purified protease IV was added to the protoplasts followed by incubation for 10 minutes before the cells were harvested for MAPK assays and *rack1* gene silencing confirmation by RT-qPCR.

For estradiol-induced *rack1* silencing in transgenic *amiR-rack1-es* lines, the wild-type Col-0 and transgenic plants were grown in MS medium in a 24-well plate as described above for 3 days. Then the medium was changed to MS medium containing 10  $\mu\text{M}$  estradiol (Sigma, 100 mM stock in DMSO). After exposure to estradiol for 2 days, the seedlings were treated with water and 40 nM flg22 or 40 nM purified protease IV for 10 minutes (MAPK assay) or 20 nM flg22 or 20 nM purified protease IV for 6 hours (RT-qPCR measuring transcript levels of *CYP71A12*, *GST6* and the three *rack1* genes). For the protease IV-mediated



protection assay against *P. syringae* DC3000, 20  $\mu$ M estradiol was infiltrated into 4-week old control Col-0 and transgenic *amiR-rack1-es1* and *amiR-rack1-es2* leaves 24 hour prior to the mock treatment or treatment with 500 nM purified protease IV.

### Mutant seed stocks

T-DNA insertion lines *gpa1-4* (CS6534), *agb1-2* (CS6536), *agg1-1c* (CS16550), *agg2-1* (SALK\_022447), *gpa1-4/agb1-2* (CS6535), *agg1-1c/agg2-1* (CS16551), *mekk1* (SALK\_052557), *rack1a-3* (CS862351), *rack1b-2* (SALK\_145920), *rack1b-3* (CS863092), *rack1c-2* (SALK\_017913), and *rack1c-3* (SALK\_001973) were obtained from the Arabidopsis Biological Resource Center.

### GUS histochemical assay

After treatment with 100 nM flg22 or 100 nM purified protease IV for 6 hours, plants were washed with 50 mM sodium phosphate (pH 7) and 0.5 mL of GUS substrate solution (50 mM sodium phosphate, pH 7, 10 mM EDTA, 0.5 mM  $K_4[Fe(CN)_6]$ , 0.5 mM  $K_3[Fe(CN)_6]$ , 0.5 mM X-Gluc, and 0.1% v/v Triton X-100) was added to each well. The plants were vacuum-infiltrated for 5 minutes and then incubated at 37°C for 4 hours. Tissues were fixed with a 3:1 ethanol:acetic acid solution at 4°C overnight and placed in 95% ethanol. Tissues were cleared in lactic acid and then examined using a Discovery V12 microscope (Zeiss). For the screen of PA14 secretome fractions, 100  $\mu$ L of buffer A (20 mM Tris, pH 8.8) or different DEAE fractions were added to each well.

### MAP kinase activity

Total proteins in seedling or protoplast lysates were resolved on a 10% SDS PAGE gel and transferred to a PVDF membrane. Western blot analysis was conducted by using anti-phospho ERK antibodies (Cell Signaling) as the primary antibody at 1:10,000 dilution in 5% BSA and HRP-conjugated anti-rabbit antibodies as the secondary antibody at 1:10,000 dilution in 5% non-fat milk. The immunoblot signal was visualized by using the SuperSignal West Femto kit (Thermo Scientific).

### Oxidative burst measurement

$H_2O_2$  was detected using a luminol-HRP (horseradish peroxidase) based chemiluminescence assay. A 10 mg/mL 500 $\times$  HRP (Sigma-Aldrich) stock solution was prepared by dissolving 10 mg HRP in water. A 20 mg/mL 500 $\times$  luminol (Sigma-Aldrich) stock solution was prepared by dissolving 20 mg luminol in 100 mM KOH. For each elicitor, a master reaction mixture was prepared by diluting individual elicitor, HRP and luminol stocks with water. The plates were kept in the dark for 1 hour before elicitation. The following procedures were carried out in the dark. Liquid was removed at the end of the 1-hour pretreatment and 200  $\mu$ L of master reaction mixture was added into each well. Plates were placed into a 96-well scintillation reader immediately and light emission was monitored using a 96-well scintillation counter (1450 Microbeta Wallac TriLux Scintillation/Luminescence counter). Every plate was read for about 30 cycles. Kinetics of  $H_2O_2$  production was determined by plotting the average chemiluminescence counts from all the seedlings under the same condition over the reading period. Every time point is the mean value of 16 seedlings.

## RNA isolation and microarray and RT-qPCR analysis

Total RNA was isolated according to the manufacturer's instructions using the RNeasy Plant Mini Kit (Qiagen). DNA was removed using the DNA-free kit (Ambion), and reverse transcription reactions were carried out using the iScript cDNA synthesis kit (Bio-Rad). cDNA concentrations were measured using a Nano-drop instrument (Thermo Scientific). RT-qPCR was carried out using a CFX96 real-time PCR machine (Bio-Rad) using iQ SYBR Green Supermix (Bio-Rad). The following PCR reaction program was used: 95°C for 3 minutes followed by 50 cycles of 95°C for 30 seconds and 55°C for 30 seconds. Fold-change was calculated relative to plants treated with M9 buffer. Fold induction data represent the mean  $\pm$  s.d.,  $n = 3$  with each containing 8 seedlings. Expression values were normalized to that of the eukaryotic translation initiation factor 4A1 (*EIF4A1*). The primers used were: *EIF4A1* (At3g13920), 5'-GCAGTCTCTTCGTGCTGACA-3' and 5'-TGTCATAGATCTGGTCCTTGAA-3'; *CYP71A12* (At2g30750), 5'-GATTATCACCTCGGTTTCCT-3' and 5'-CCACTAATACTTCCCAGATTA-3'; *WRKY30* (At5g24110), 5'-GCAGCTTGAGAGCAAGAATG-3' and 5'-AGCCAAATTTCCAAGAGGAT-3'; *GST6* (At2g47730), 5'-CCATCTTCAAAGGCTGGAAC-3' and 5'-TCGAGCTCAAAGATGGTGAA-3'; *WRKY29* (At4g23550), 5'-ATCCAACGGATCAAGAGCTG-3' and 5'-GCGTCCGACAACAGATTCTC-3'; *WRKY33* (At2g38470), 5'-GGGAAACCCAAATCCAAGA-3' and 5'-GTTCCCTTCGTAGGTTGTGA-3'; *ERF1* (At3g23240), 5'-TCGGCGATTCTCAATTTTTC-3' and 5'-ACAACCGGAGAACAACCATC-3'; *rack1a* (At1g18080), 5'-GCTGAAAAGGCTGACAACAGT-3' and 5'-GCTCCAGTTAAGGCTTGTGC-3'; *rack1b* (At1g48630), 5'-TTGTTGAGGATTTGAAGGTTGA-3' and 5'-CCAGTTCAAGCTTGTGCAGTA-3'; *rack1c* (At3g18130), 5'-GAGGCAGAGAAGAATGAAGGTG-3' and 5'-CCAGTTCAAGCTTGTGCAGTA-3'. *WRKY* gene induction was measured 1 hour after elicitation, whereas *CYP71A12*, *ERF1*, and *GST6*, were measured 6 hours after elicitor treatment.

For microarray analysis, RNA quality was assessed by checking the integrity of RNA on an Agilent 2100 Bioanalyzer (Agilent Technologies). Target labeling was performed according to the protocol given in the Affymetrix GeneChip 3' IVT Express Kit Technical Manual. Microarray hybridizations and scanning were finished at the Genomics Core, Joslin Diabetes Center, Boston, MA. Microarray CEL files were read into the R statistical analysis software, version 2.15.2. Arrays were analyzed together using the standard RMA procedure as implemented in Bioconductor's "affy" package, version 1.36.1<sup>32,33</sup>. Fold changes were calculated using log-base-2-transformed expression values by subtracting the mean of control samples from the mean of treated samples. Microarray CEL files were also obtained from previous studies exploring the effects of flg22 and OGs on gene expression<sup>4</sup>. These two experiments were subjected to the RMA procedure together, but downstream analyses (e.g. fold change computations) were performed separately on the two treatments. The microarray data has been deposited in the GEO database under the submission number: GSE58518.

### Callose deposition assay

Elicitor-induced callose deposition in cotyledons of 10-day old *Arabidopsis* seedlings was detected using aniline blue as described<sup>34</sup>. Eighteen hours after elicitation, seedlings were fixed under a vacuum in 3:1 ethanol:acetic acid. The clearing solution was changed until the leaves were colorless. Tissues were washed in 70% ethanol and then 50% ethanol for at least 2 hours each time and rehydrated in several brief H<sub>2</sub>O washes followed by an overnight H<sub>2</sub>O wash. Samples were then made transparent by several minutes in a vacuum with 10% NaOH followed by a 2-hour incubation at 37°C on a shaking platform. After several more H<sub>2</sub>O washes, tissues were incubated in the dark at room temperature for at least 4 hours with 0.01% aniline blue in 150 mM K<sub>2</sub>HPO<sub>4</sub> (pH 9.5). After mounting on slides in 50% glycerol, samples were examined using a Zeiss Axioplan microscope (Oberkochen, Germany) utilizing UV illumination and a broadband DAPI filter set (excitation filter 390 nm; dichroic mirror 420 nm; emission filter 460 nm).

### Pathogenicity assays

*Arabidopsis* pathogenicity assays, including infection by *P. syringae* strain DC3000 with or without pre-infiltration of protease IV or flg22, were performed according to previously described protocols<sup>21</sup>. Data represent the mean of bacterial titers  $\pm$  s.d. of ten leaf disks excised from 10 leaves of 5 plants. The infection protection assay was repeated three times with similar results.

*Xanthomonas* pathogenicity assays in *Brassica oleracea* were carried out according to previously described protocols<sup>35</sup> with modifications. Seeds of broccoli cultivar *B. oleracea* var. Marathon were sown in Fafard #2 soil mix and grown in a 12-hour light (70  $\mu\text{E}\cdot\text{m}^{-2}\cdot\text{s}^{-1}$ ) cycle at 19°C and 60% relative humidity. Individual seedlings were transferred to 5  $\times$  5 cm pots after one week and kept at a cycle of 16-hour light (150  $\mu\text{E}\cdot\text{m}^{-2}\cdot\text{s}^{-1}$ ) at 23°C followed by 8-hour dark at 20°C and 70% relative humidity. After a further two weeks of growth, the three-week old plants were used for *Xanthomonas* infiltration. Fresh *X. campestris* overnight cultures were washed and adjusted to 10<sup>6</sup> cells/ml in 10 mM MgSO<sub>4</sub>. A standard infiltration protocol was used to infect 3-week old leaves. After infection, the plants were transferred to a growth chamber with the following conditions: 12-hour light (60  $\mu\text{E}\cdot\text{m}^{-2}\cdot\text{s}^{-1}$ ) at 28°C at 90% relative humidity for two days before being harvested for CFU counting. Data represent the mean of bacterial titers  $\pm$  s.d. of ten leaf disks excised from 10 leaves of 5 plants. The infection protection assay was repeated three times with similar results.

### Co-immunoprecipitation (co-IP)

For co-IP carried out in protoplasts, mesophyll protoplast isolation from leaves of 4-week old *Arabidopsis* plants and polyethylene glycol (PEG)-mediated DNA transfection were carried out as previously described<sup>36</sup>. Co-IP was performed as described previously<sup>37</sup> with modifications. Briefly, 100  $\mu\text{g}$  (50  $\mu\text{L}$ ) of PREY plasmids were used to co-transfect 1 mL *Arabidopsis* mesophyll protoplasts ( $5\times 10^5$  cells) with 100  $\mu\text{g}$  (50  $\mu\text{L}$ ) of BAIT plasmids or empty vectors. After 6 hours to allow protein expression, the cells were pelleted and lysed in 200  $\mu\text{L}$  of IP buffer (10 mM HEPES, pH7.5, 150 mM NaCl, 1 mM EDTA, 10% glycerol, 1% Triton X-100, 1 $\times$  Roche EDTA-free protease inhibitor cocktail) by vigorous vortexing

for 1 min. Twenty  $\mu\text{L}$  of lysate was saved as the input fraction to ensure that the Prey proteins were expressed equally in all samples. The rest of the lysate (180  $\mu\text{L}$ ) was mixed with 320  $\mu\text{L}$  IP buffer and vigorously vortexed for 1 min. The resultant clear lysate was centrifuged at  $21,000 \times g$  for 10 min at  $4^\circ\text{C}$ , and the supernatant was incubated with a 10  $\mu\text{L}$  slurry of anti-FLAG M2 agarose beads (Sigma) or anti-HA magnetic beads (Pierce) for 3 hr at  $4^\circ\text{C}$ . The beads were washed 3 times with the IP buffer and once with 50 mM Tris-HCl, pH7.5. The eluate was obtained by boiling the beads in 40  $\mu\text{L}$  of SDS-PAGE loading buffer and the presence of Co-IPed PREY proteins was detected by immunoblotting analysis using HRP-conjugated anti-HA antibody or anti-FLAG (Roche) at 1:10,000 dilution, and the immunoblot signal was visualized using the SuperSignal West Femto kit (Thermo Scientific). The same membrane was stripped and re-used to detect the comparable amounts of IPed BAIT proteins by immunoblot.

### Bimolecular fluorescence complementation (BiFC)

For plasmids used in the split-mCherry assay, the coding sequence of the N-terminal fragment (mCherryN, aa1- aa159) or the C-terminal fragment (mCherryC, aa160-aa235) of mCherry was PCR amplified, digested by *Bam*HI/*Not*I, and inserted into the same digested pAN vector, which contains a double 35S promoter and a NOS terminator, to obtain pcCherryN and pcCherryC plasmids. Genes for protein-protein interaction tests were inserted into the *Xba*I/*Bam*HI digested pcCherryN or pcCherryC vectors after digestion of their PCR products with *Xba*I (or *Spe*I, *Nhe*I if the *Xba*I site was present in the gene) at the 5' end and with *Bam*HI (or *Bgl*II if the *Bam*HI site was present in the gene) at the 3' end, allowing the expression of a chimeric gene of interest with the coding sequence of mCherryN or mCherryC at the 3' end.

For binary plasmids used in the BiFC assay in Agroinfiltrated *Nicotiana benthamiana* leaves, pFGC-RCS (kanamycin resistant) and pPZP-RCS (spectinomycin resistant) binary vectors were constructed by replacing the original sequences between *Eco*RI and *Hind*III of pFGC19 and pPZP222 with the multiple cloning site sequence from pUC119-RCS flanked by *Eco*RI and *Hind*III<sup>38</sup>. Subsequently, the entire expression cassette of “gene”-mCherryN was PCR amplified from protoplast expression plasmids, digested by *Asc*I and inserted into the *Asc*I site of pFGC-RCS, while the entire expression cassette containing the “gene”-mCherryC fusion DNA was PCR amplified from protoplast expression plasmids, digested by *Asc*I and inserted into the *Asc*I site of pPZP-RCS. A pair of pFGC-RCS and pPZP-RCS plasmids expressing a pair of genes for protein-protein interaction tests were co-transformed into *Agrobacterium* GV3101 cells by electroporation, and cells transformed with both binary plasmids were selected by the addition of both kanamycin and spectinomycin to the growth medium. Leaves of 4- to 5-week old *N. benthamiana* plants were infiltrated with agrobacteria (final  $\text{OD}_{600} = 0.01$ ) containing constructs expressing the mCherryN fragment fused to GPA1, AGB1 or MAP kinases and the mCherryC fragment fused to RACK1A/B/C. The agroinfiltration experiment was carried out as described previously<sup>39</sup>.

*Arabidopsis* protoplasts 18 hours after transfection and *N. benthamiana* leaf pieces 2 days after agroinfiltration were imaged using a Leica DM-6000B upright fluorescence

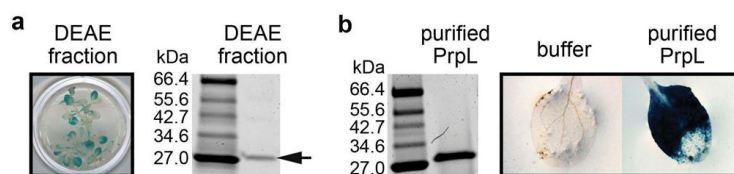
microscope with phase and differential interference contrast equipped with a Leica FW4000 digital image-acquisition and processing system.

### Split firefly luciferase complementation (SFLC)

For plasmids used in the SFLC assay, the genes for protein-protein interaction tests were inserted into the *XbaI/BamHI* digested pcFLucN or pcFLucC vectors<sup>37</sup> after digestion of their PCR products with *XbaI* (or *SpeI*, *NheI* if the *XbaI* site is present in the gene) at the 5' end and with *BamHI* (or *BglII* if the *BamHI* site is present in the gene) at the 3' end, allowing the expression of a chimeric gene of interest with the coding sequence of FLucN or FLucC at the 3' end.

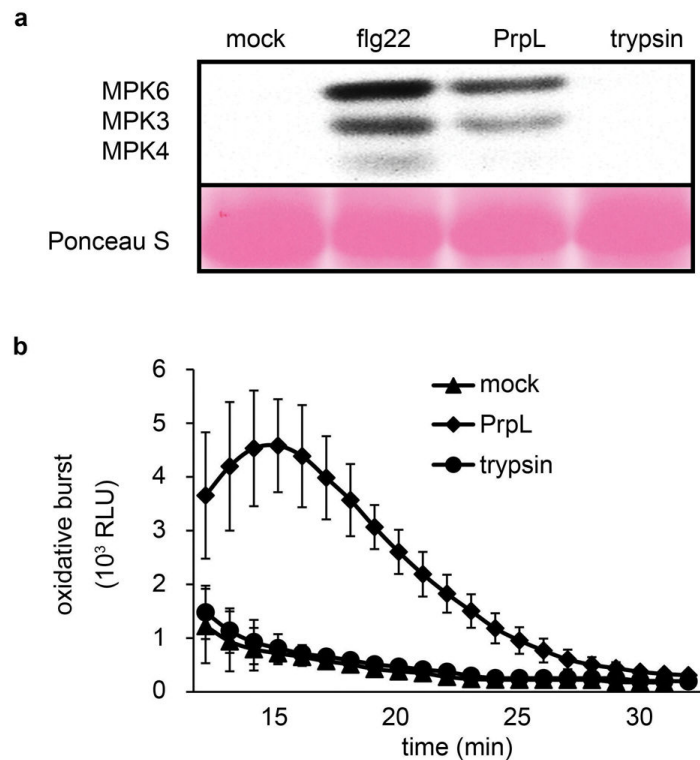
SFLC experiments carried out in protoplasts were performed as described previously<sup>37</sup>. Briefly, 10  $\mu\text{g}$  (5  $\mu\text{L}$ ) of PREY plasmids were used to co-transfect 100  $\mu\text{L}$  of *Arabidopsis* mesophyll protoplasts ( $5 \times 10^5$  cells) with 10  $\mu\text{g}$  (5  $\mu\text{L}$ ) of BAIT plasmids. One  $\mu\text{g}$  UBQ10::GUS plasmid was used in each transfection as an internal normalization control. After 6 hours to allow for protein expression, the luminescence of each sample was recorded by a GloMax-Multi microplate multimode reader (Promega) with the integration time set as 1 sec.

### Extended Data



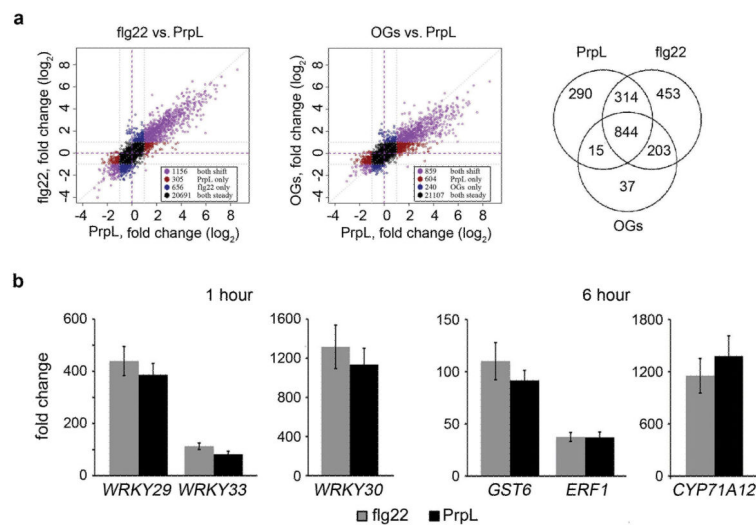
**Extended Data Figure 1. Protease IV-triggered GUS staining in *CYP71A12pro:GUS* transgenic *Arabidopsis* seedlings**

**a**, Activation of *CYP71A12pro:GUS* by a DEAE fraction of the PA14 secretome (left) and purification of the eliciting activity by DEAE chromatography (right). **b**, Activation of *CYP71A12pro:GUS* in 10-day old seedlings by 100 nM purified PrpL. The experiments in panels **a** and **b** were repeated three times with similar results.



**Extended Data Figure 2. Trypsin does not activate MAPK cascade or elicit an oxidative burst in *Arabidopsis*.**

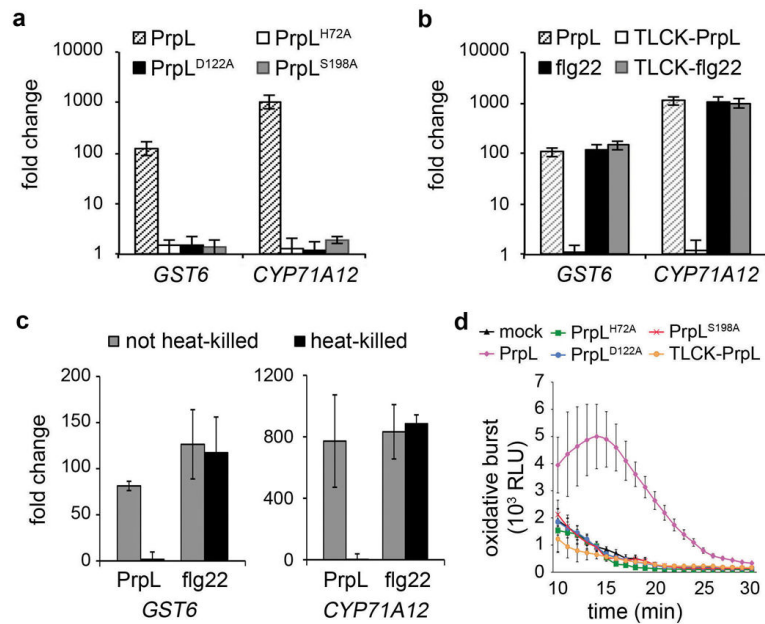
**a**, Western blot depicting activation of MAPKs by 40 nM flg22, or 40 nM purified PrpL, or trypsin in 10-day old seedlings. The same molecular weight region of the Western blot is shown as in Fig. 1b. **b**, Chemiluminescence assay showing elicitation of an oxidative burst in 10-day old seedlings by 20 nM purified PrpL or trypsin. Error bars represent standard deviation;  $n = 16$  individual seedlings.



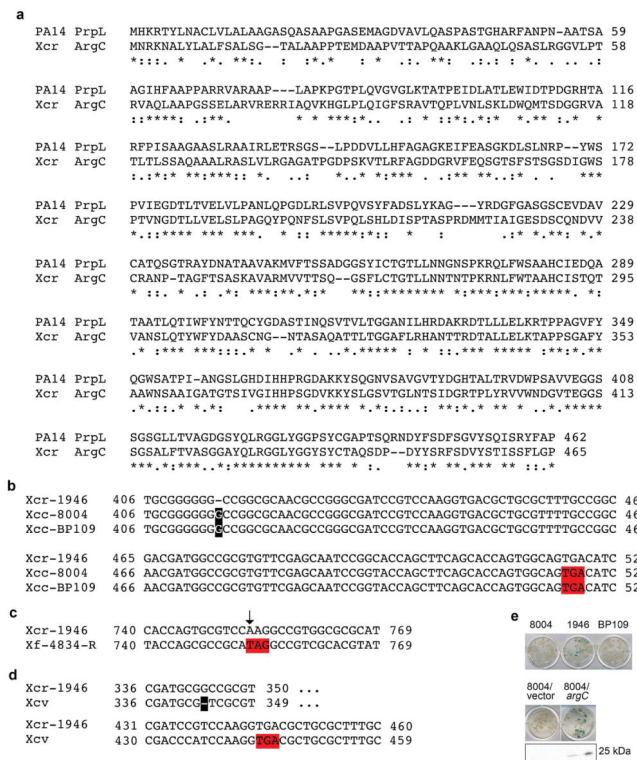
**Extended Data Figure 3. Transcriptional analysis of purified protease IV**



**a**, Genome-wide transcriptomic profiles obtained with Affymetrix Arabidopsis ATH1 GeneChips® of 10-day old seedlings treated with 20 nM purified PrpL and comparison to published flg22- and oligogalacturonide (OG)-responses. A Venn diagram shows the similarity of expression behavior ( $|\text{fold change}| > 2$ ) in response to the three treatments. **b**, Defense gene induction levels measured by RT-qPCR in 10-day old Col-0 seedlings treated with 20 nM purified PrpL or 20 nM flg22 for 1 hour (*WRKY29*, *30*, and *33*) or 6 hours (*GST6*, *ERF1*, and *CYP71A12*). The data represent the mean  $\pm$  s.d.,  $n = 3$  biological replicates, each containing 8 seedlings.

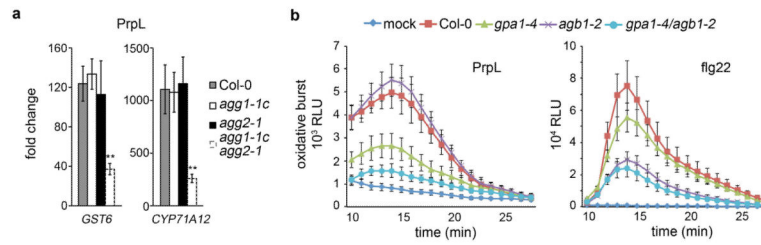


**Extended Data Figure 4. Protease IV-triggered responses are dependent on proteolytic activity**  
**a**, Induction of defense-related genes by 20 nM purified PrpL or inactive variants of PrpL measured by RT-qPCR. **b**, Induction of defense-related genes by 20 nM purified PrpL or 20 nM flg22, or 20 nM TLCK-treated PrpL or 20 nM TLCK-treated flg22 measured by RT-qPCR. **c**, Induction of defense-related genes by 20 nM PrpL or 20 nM heat-treated PrpL or 20 nM flg22 or 20 nM heat-treated flg22 measured by RT-qPCR. **d**, Chemiluminescence assay showing elicitation of an oxidative burst by 20 nM purified PrpL, 20 nM inactive variants of PrpL, or 20 nM TLCK-treated PrpL. The data represent the mean  $\pm$  s.d.,  $n = 3$  biological replicates with each experiment contains eight seedlings (**a**, **b**, **c**), and  $n = 16$  individual seedlings (**d**).



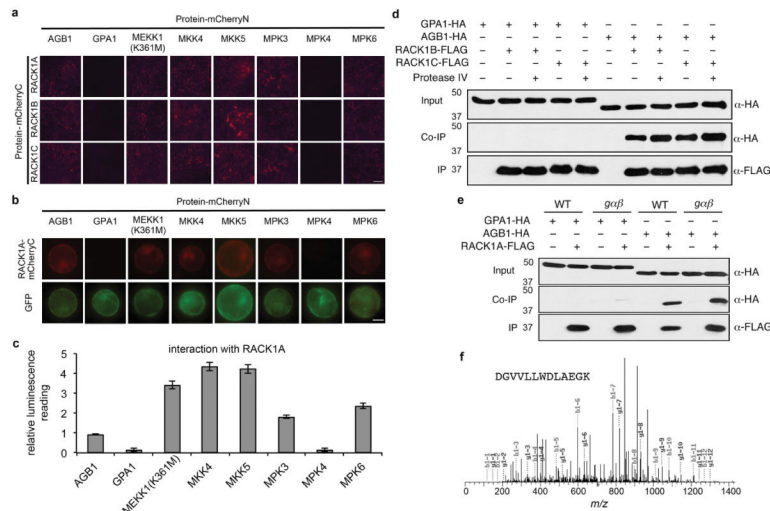
**Extended Data Figure 5. Sequence analyses of *Xanthomonas argC* genes**  
**a**, The protein sequence alignment between *P. aeruginosa* PA14 PrpL and *X. campestris* pv. *raphani* strain 1946 ArgC (Xcr ArgC). **b to d**, Three independent presumptive null mutations in the *Xanthomonas argC* gene: an insertion of G, a single nucleotide mutation, and a deletion. The extra G is highlighted in black in **b**; the single nucleotide substitution is indicated by an arrow in **c**; and the single base deletion is highlighted in black in **d**. The resulting premature stop codons are highlighted in red. Sequences were aligned to the *argC* allele in *X. campestris* pv. *raphani* strain 1946 (Xcr-1946), from which the *argC* gene was cloned. *X. campestris* pv. *campestris* strains 8004 (Xcc-8004); *X. campestris* pv. *campestris* strains BP109 (Xcc-BP109); *X. fuscans* subsp. *fuscans* strain 4834-R (Xf-4834-R); *X. campestris* pv. *vesicatoria* (Xcv). **e**. Activation of *CYP71A12pro:GUS* in 10-day old seedlings by culture filtrate from *X. campestris* strain Xcr-1946, Xcc-8004, or Xcc-BP109, and *X. campestris* strain 8004 complemented with a functional *argC* gene (8004/*argC*) or transformed with empty vector (8004/vector). Detection of HA-ArgC with an anti-HA antibody. The GUS staining was repeated three times with similar results and the representative images shown were selected from at least three images.

Author Manuscript



### Extended Data Figure 6. G proteins are required for protease IV response

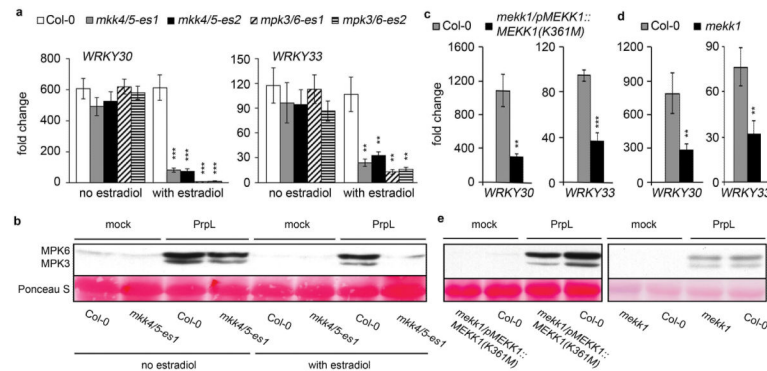
**a**, Induction of *CYP71A12* and *GST6* gene expression by 20 nM purified PrpL in 10-day old wild-type Col-0, *gyl* single mutants (*agg1-1c* and *agg2-1*), or a *gyl*  $\gamma 2$  double mutant measured by RT-qPCR. **b**, Chemiluminescence assay showing elicitation of an oxidative burst by 20 nM purified PrpL or 20 nM flg22 in wild-type Col-0 or G protein T-DNA mutants. The data represent the mean  $\pm$  s.d.,  $n = 3$  biological replicates with each containing 8 seedlings (**a**), and  $n = 16$  individual seedlings (**b**); \*\* $P < 0.01$ , Student's *t*-test.



### Extended Data Figure 7. Interactions between RACK1 and G $\beta$ or MAP kinases

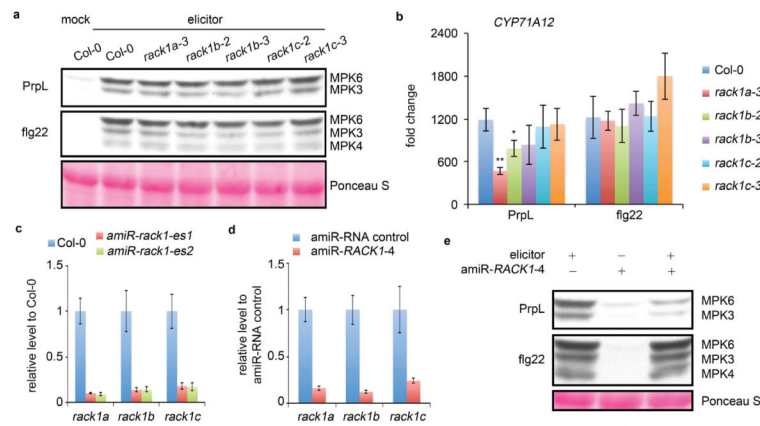
**a**, Split-mCherry assay in 4-week old *Agrobacterium*-infiltrated *Nicotiana benthamiana* leaves. Images were pseudocolored for visualization. Bar = 100  $\mu$ m. RACK1A, B, C proteins were fused with the C-terminal half of mCherry and the potential interaction partner proteins were fused with the N-terminal half of mCherry. **b**, Split-mCherry assay in *Arabidopsis* protoplasts. RACK1A protein was fused with the C-terminal half of mCherry and the potential interaction partner proteins were fused with the N-terminal half of mCherry. GFP protein was included in each experiment to serve as a transfection control. Images were pseudocolored for visualization. Bar = 10  $\mu$ m. **c**, Relative interaction intensity between RACK1A and G proteins or MAP kinases measured by split firefly luciferase complementation. RACK1A protein was fused with the FLucN or FLucC to pair with G proteins or MAP kinases fused with the other half of firefly luciferase. Both constructs were co-expressed in protoplasts for 6 h and the complemented luciferase activity was used to relatively quantify protein-protein interactions. UBQ10::GUS was included in each experiment to serve as a transfection normalization control. The data represent the mean  $\pm$

s.d.,  $n = 3$  technical replicate samples. **d**, Protoplasts were co-transfected with GPA1-HA or AGB1-HA and RACK1B/C-FLAG or a control vector. Co-IP was carried out with an anti-FLAG antibody. (Top) The expression of GPA1 or AGB1 protein. (Middle) AGB1, but not GPA1 co-immunoprecipitates with RACK1 proteins. (Bottom) Pull-down of RACK1 proteins by anti-FLAG antibody. Protoplasts were treated with 100 nM purified PrpL for 15 min. **e**, Co-IP between GPA1 or AGB1 and RACK1A was carried out in wild-type Col-0 or *gab* mutant *Arabidopsis* mesophyll protoplasts. Numbers left of blots represent marker size in kDa. **f**, Mass spectrophotometric analysis of endogenous proteins pulled down by FLAG-tagged MEKK1(K361M). A peptide conserved in all three RACK1 proteins is shown. The experiments in panels **a** and **b** were repeated three times with similar results.



#### Extended Data Figure 8. Protease IV-triggered defense responses in wild-type Col-0 and MAP kinase mutants

**a**, Induction of *WRKY30* and *WRKY33* gene expression by 20 nM purified PrpL in 7-day old seedlings of wild-type Col-0 and transgenic *mpk3,6-es1/2* and *mkk4,5-es1/2* plants in the absence or presence of estradiol. **b**, Western blot depicting activation of MPK3 and MPK6 by 40 nM purified PrpL in 7-day old seedlings of wild-type Col-0 and transgenic *mkk4,5-es1* plants in the absence or presence of estradiol. The same molecular weight region of the Western blot is shown as in Fig. 1b. **c**, Induction of *WRKY30* and *WRKY33* gene expression by 20 nM purified PrpL in 10-day old wild-type Col-0 and *mekk1/pMEKK1::MEKK1(K361M)* mutant seedlings. **d**, Induction of *WRKY30* and *WRKY33* gene expression by 20 nM purified PrpL in 4-day old wild-type Col-0 and *mekk1* null mutant seedlings. **e**, Western blot depicting activation of MPK3 and MPK6 by 40 nM purified PrpL in 10-day old wild-type Col-0 and *mekk1/pMEKK1::MEKK1(K361M)* mutant seedlings or 4-day old wild-type Col-0 and *mekk1* null mutant seedlings. The same molecular weight region of the Western blot is shown as in Fig. 1b. The data represent the mean  $\pm$  s.d.,  $n = 3$  biological replicates with each containing 8 seedlings (**a**, **c**, **d**); \*\* $P < 0.01$ ; \*\*\* $P < 0.001$ , Student's *t*-test vs. Col-0 controls.



### Extended Data Figure 9. RACK1 proteins are required for protease IV response

**a**, Western blot depicting activation of MAPKs by 40 nM purified PrpL or 40 nM flg22 in 5-day old seedlings of wild-type Col-0 and individual *rack1*::T-DNA insertion mutants. The same molecular weight region of the Western blot is shown as in Fig. 1b. **b**, Induction of *CYP71A12* by 20 nM purified PrpL or 20 nM flg22 in 5-day old seedlings of wild-type Col-0 and individual *rack1*::T-DNA insertion mutants. **c**, RT-qPCR analysis of *rack1a*, *rack1b*, and *rack1c* transcript levels in the 5-day old Col-0 or *amiR-rack1-es1* and *amiR-rack1-es2* seedlings. **d**, RT-qPCR analysis of *rack1a*, *rack1b*, and *rack1c* transcript levels in *Arabidopsis* protoplasts transfected with *amiR-RACK1-4* or *amiRNA* control. **e**, Western blot depicting activation of MAPKs by 40 nM purified PrpL or 40 nM flg22 in *Arabidopsis* protoplasts transfected with *amiR-RACK1-4* or *amiRNA* control. The same molecular weight region of the Western blot is shown as in Fig. 1b. The data represent the mean  $\pm$  s.d.,  $n = 3$  biological replicates (**b**, **c**, **d**); \* $P < 0.05$ ; \*\* $P < 0.01$ , Student's *t*-test.

Extended Data Table 1

*P. aeruginosa* PA14 transposon mutants screened for activation of *CYP71A12pro:GUS*.

gene names	gene IDs	type*	gene names	gene IDs	type*	gene names	gene IDs	type*
<i>aprA</i>	865	1	<i>toxA</i>	399	2	<i>cIpB</i>	130	6
<i>aprD</i>	7385	1	<i>xcpP</i>	3450	2	<i>hcp1</i>	4311	6
<i>aprE</i>	1317	1	<i>xcpQ</i>	417	2	<i>hcpA</i>	4107	6
<i>aprF</i>	922	1	<i>xcpR</i>	812	2	<i>stnR</i>	1865	6
<i>aprI</i>	4760	1	<i>xcpT</i>	4498	2	<i>stp1</i>	3334	6
<i>aprX</i>	1421	1	<i>xcpW</i>	3292	2	<i>vgrG2</i>	141	6
<i>hasAp</i>	3774	1	<i>xcpZ</i>	4249	2	<i>gacA</i>	631	R
<i>hasF</i>	1253	1	<i>xphA</i>	4239	2	<i>lasI</i>	3828	R
<i>cbpD</i>	1394	2	<i>xqhA</i>	246	2	<i>rhII</i>	3829	R
<i>cupB5</i>	75	2	<i>exoT</i>	7001	3	<i>rhIR</i>	3229	R
<i>lasA</i>	1299	2	<i>exoU</i>	339	3	<i>rpoS</i>	2108	R
<i>lasB</i>	759	2	<i>exoY</i>	7430	3	<i>fimL</i>	627	S
<i>lipA</i>	2386	2	<i>pseD</i>	1303	3	<i>flgB</i>	4759	S

gene names	gene IDs	type*	gene names	gene IDs	type*	gene names	gene IDs	type*
<i>lipC</i>	2417	2	<i>aaaA</i>	375	5	<i>flgK</i>	352	S
<i>pepB</i>	629	2	<i>eprS</i>	69	5	<i>fliC</i>	1029	S
<i>phoA</i>	914	2	<i>estA</i>	354	5	<i>fliN</i>	4482	S
<i>phoB</i>	3473	2	<i>lepA</i>	631	5	<i>motA</i>	2879	S
<i>phoR</i>	1112	2	<i>tps1</i>	556	5	<i>motB</i>	1935	S
<i>plcB</i>	1956	2	<i>tps2</i>	600	5	<i>pilA</i>	7353	S
<i>plcH</i>	210	2	<i>tps3</i>	555	5	<i>pilD</i>	2579	S
<i>plcN</i>	267	2	<i>tps5</i>	545	5	<i>tadZ</i>	1689	S
<i>pmpA</i>	93	2						

\*Numbers represent the type of secretion system. For example, 2 means Type II secreted protein or Type II secretion machinery protein. R represents regulatory proteins. S represents surface proteins.

## Supplementary Material

Refer to Web version on PubMed Central for supplementary material.

## Acknowledgments

We thank G. Tena for generating the *mekk1/pMEKK1::MEKK1(K361M)* transgenic line, Y. Zhang for the *sum1-1* mutant, M.C. Suarez-Rodriguez and P.J. Krysan for discussion, the Arabidopsis Biological Resource Center for T-DNA insertion lines, and M. Curtis and U. Grossniklaus for the estradiol-inducible binary vector. We thank S. Lory for *P. aeruginosa* PAO ADD1976, M.B. Mudgett for pVSP61. We thank N. Clay, X. Dong, S. Somerville, and Ausubel lab members for critical reading of the manuscript. This work was supported by NSERC and Banting Postdoctoral Fellowships awarded to Z.C., NSF grants MCB-0519898 and IOS-0929226 and NIH grants R37-GM48707 and P30 DK040561 awarded to F.M.A., and NSF grant IOS-0618292 and NIH grant R01-GM70567 awarded to J.S.

## References

1. Tena G, Boudsocq M, Sheen J. Protein kinase signaling networks in plant innate immunity. *Curr. Opin. Plant Biol.* 2011; 14:519–529. [PubMed: 21704551]
2. Arthur JS, Ley SC. Mitogen-activated protein kinases in innate immunity. *Nat. Rev. Immunol.* 2013; 13:679–692. [PubMed: 23954936]
3. Millet YA, et al. Innate immune responses activated in Arabidopsis roots by microbe-associated molecular patterns. *Plant Cell.* 2010; 22:973–990. [PubMed: 20348432]
4. Denoux C, et al. Activation of defense response pathways by OGs and flg22 elicitors in Arabidopsis seedlings. *Mol. Plant.* 2008; 1:423–445. [PubMed: 19825551]
5. Traidej M, Marquart ME, Caballero AR, Thibodeaux BA, O'Callaghan RJ. Identification of the active site residues of *Pseudomonas aeruginosa* protease IV. *J. Biol. Chem.* 2003; 278:2549–2553. [PubMed: 12419815]
6. Urano D, Chen J-G, Botella JR, Jones AM. Heterotrimeric G protein signalling in the plant kingdom. *Open Biol.* 2013; 3:120186. [PubMed: 23536550]
7. Ullah H, et al. Structure of a signal transduction regulator, RACK1, from Arabidopsis thaliana. *Protein Sci.* 2008; 17:1771–1780. [PubMed: 18715992]
8. Dell EJ, et al. The betagamma subunit of heterotrimeric G proteins interacts with RACK1 and two other WD repeat proteins. *J. Biol. Chem.* 2002; 277:49888–49895. [PubMed: 12359736]
9. Nakashima A, et al. RACK1 functions in rice innate immunity by interacting with the Rac1 immune complex. *Plant Cell.* 2008; 20:2265–2279. [PubMed: 18723578]



10. Chen J-G, et al. RACK1 mediates multiple hormone responsiveness and developmental processes in Arabidopsis. *J. Exp. Bot.* 2006; 57:2697–2708. [PubMed: 16829549]
11. Asai T, et al. MAP kinase signalling cascade in Arabidopsis innate immunity. *Nature.* 2002; 415:977–983. [PubMed: 11875555]
12. Suarez-Rodriguez MC, et al. MEKK1 is required for flg22-induced MPK4 activation in Arabidopsis plants. *Plant Physiol.* 2007; 143:661–669. [PubMed: 17142480]
13. Ichimura K, et al. (MAPK Group). Mitogen-activated protein kinase cascades in plants: a new nomenclature. *Trends Plant Sci.* 2002; 7:301–308. [PubMed: 12119167]
14. Guo J, Chen J-G. RACK1 genes regulate plant development with unequal genetic redundancy in Arabidopsis. *BMC Plant Biol.* 2008; 8:108. [PubMed: 18947417]
15. Li J-F, et al. Comprehensive protein-based artificial microRNA screens for effective gene silencing in plants. *Plant Cell.* 2013; 25:1507–1522. [PubMed: 23645631]
16. Witzel F, Maddison L, Blüthgen N. How scaffolds shape MAPK signaling: what we know and opportunities for systems approaches. *Front. Physiol.* 2012; 3:475. [PubMed: 23267331]
17. Rahme LG, et al. Common virulence factors for bacterial pathogenicity in plants and animals. *Science.* 1995; 268:1899–1902. [PubMed: 7604262]
18. Liberati NT, et al. An ordered, nonredundant library of *Pseudomonas aeruginosa* strain PA14 transposon insertion mutants. *Proc. Natl. Acad. Sci. U.S.A.* 2006; 103:2833–2838. [PubMed: 16477005]
19. Motley ST, Lory S. Functional characterization of a serine/threonine protein kinase of *Pseudomonas aeruginosa*. *Infect. Immun.* 1999; 67:5386–5394. [PubMed: 10496921]
20. Parker JE, Barber CE, Mi-jiao F, Daniels MJ. Interaction of *Xanthomonas campestris* with *Arabidopsis thaliana*: Characterization of a gene from *X. c. pv. raphani* that confers avirulence to most *A. thaliana* accessions. *Mol. Plant-Microbe Interact.* 1993; 6:216–224. [PubMed: 8471795]
21. Djonovi S, et al. Trehalose biosynthesis promotes *Pseudomonas aeruginosa* pathogenicity in plants. *PLoS Pathog.* 2013; 9:e1003217. [PubMed: 23505373]
22. Prentki P, Krisch HM. *In vitro* insertional mutagenesis with a selectable DNA fragment. *Gene.* 1984; 29:303–313. [PubMed: 6237955]
23. Hirsch AM, et al. Rhizobium meliloti nodulation genes allow *Agrobacterium tumefaciens* and *Escherichia coli* to form pseudonodules on alfalfa. *J. Bacteriol.* 1984; 158:1133–1143. [PubMed: 6327629]
24. Cheng Z, Duan J, Hao Y, McConkey BJ, Glick BR. Identification of bacterial proteins mediating the interactions between *Pseudomonas putida* UW4 and *Brassica napus* (canola). *Mol. Plant-Microbe Interact.* 2009; 22:686–694. [PubMed: 19445593]
25. Smith AW, Iglewski BH. Transformation of *Pseudomonas aeruginosa* by electroporation. *Nucleic Acids Res.* 1989; 17:10509. [PubMed: 2513561]
26. Kim J-G, et al. *Xanthomonas* T3S effector XopN suppresses PAMP-triggered immunity and interacts with a tomato atypical receptor-like kinase and TFT1. *Plant Cell.* 2009; 21:1305–1323. [PubMed: 19366901]
27. Curtis MD, Grossniklaus U. A gateway cloning vector set for high-throughput functional analysis of genes in planta. *Plant Physiol.* 2003; 133:462–469. [PubMed: 14555774]
28. Lee L-Y, Fang M-J, Kuang L-Y, Gelvin SB. Vectors for multi-color bimolecular fluorescence complementation to investigate protein-protein interactions in living plant cells. *Plant Methods.* 2008; 4:24. [PubMed: 18922163]
29. Zuo J, Niu QW, Chua NH. Technical advance: an estrogen receptor-based transactivator XVE mediates highly inducible gene expression in transgenic plants. *Plant J.* 2000; 24:265–273. [PubMed: 11069700]
30. Clough SJ, Bent AF. Floral dip: a simplified method for *Agrobacterium*-mediated transformation of *Arabidopsis thaliana*. *Plant J.* 1998; 16:735–743. [PubMed: 10069079]
31. Engel LS, Hill JM, Caballero AR, Green LC, O'Callaghan RJ. Protease IV, a unique extracellular protease and virulence factor from *Pseudomonas aeruginosa*. *J. Biol. Chem.* 1998; 273:16792–16797. [PubMed: 9642237]

32. Irizarry RA, et al. Exploration, normalization, and summaries of high density oligonucleotide array probe level data. *Biostatistics*. 2003; 4:249–264. [PubMed: 12925520]
33. Gentleman RC, et al. Bioconductor: Open software development for computational biology and bioinformatics. *Genome Biol*. 2004; 5:R80. [PubMed: 15461798]
34. Clay NK, Adio AM, Denoux C, Jander G, Ausubel FM. Glucosinolate metabolites required for an *Arabidopsis* innate immune response. *Science*. 2009; 323:95–101. [PubMed: 19095898]
35. Meyer D, Lauber E, Roby D, Arlat M, Kroj T. Optimization of pathogenicity assays to study the *Arabidopsis thaliana* - *Xanthomonas campestris* pv. *campestris* pathosystem. *Mol. Plant Pathol*. 2005; 6:327–333. [PubMed: 20565661]
36. Yoo SD, Cho YH, Sheen J. *Arabidopsis* mesophyll protoplasts: a versatile cell system for transient gene expression analysis. *Nat. Protocols*. 2007; 2:1565–1572. [PubMed: 17585298]
37. Li J-F, Bush J, Xiong Y, Li L, McCormack M. Large-scale protein-protein interaction analysis in *Arabidopsis* mesophyll protoplasts by split firefly luciferase complementation. *PLoS One*. 2011; 6:e27364. [PubMed: 22096563]
38. Li J-F, Park E, von Arnim AG, Nebenfuhr A. The FAST technique: a simplified *Agrobacterium*-based transformation method for transient gene expression analysis in seedlings of *Arabidopsis* and other plant species. *Plant Methods*. 2009; 5:6. [PubMed: 19457242]
39. King SRF, et al. *Phytophthora infestans* RXLR effector PexRD2 interacts with host MAPKKKε to suppress plant immune signaling. *Plant Cell*. 2014; 26:1345–1359. [PubMed: 24632534]

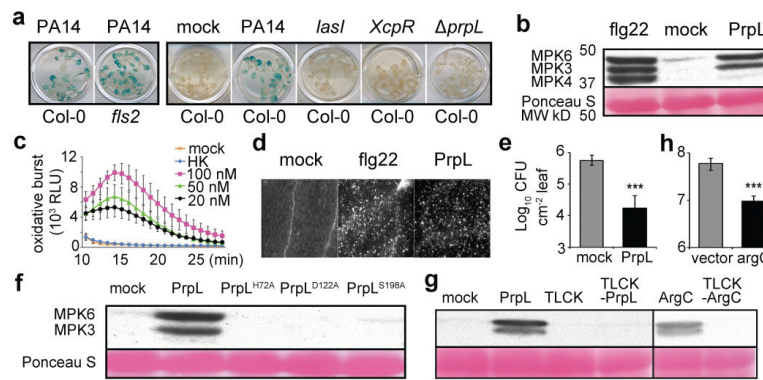


**Figure 1. Proteases trigger innate immune responses in *Arabidopsis* via proteolytic activity**  
**a**, Activation of *CYP71A12pro::GUS* in wild-type *Arabidopsis* Col-0 or *fls2* mutant cotyledons by culture filtrates from wild-type *P. aeruginosa* PA14, from PA14 mutants containing transposon insertion in *lasI* and *xcpR*, or from PA14/ *prpL*. **b**, Western blot depicting activation of MAPKs by PrpL or flg22. Numbers left of blot represent marker size in kDa. **c**, Chemiluminescence assay showing elicitation of an oxidative burst by PrpL. RLU: relative luminescence units. HK: 100 nM “heat-killed” PrpL. **d**, Callose formation in cotyledons elicited by PrpL or flg22 detected by aniline blue staining. **e**, Protection of 4-week old *Arabidopsis* leaves from *P. syringae* pv. *tomato* strain DC3000 infection by pre-infiltrated PrpL. **f**, Western blot depicting activation of MPK3 and MPK6 by PrpL and inactive variants of PrpL. The same molecular weight region of the blot is shown as in **b**. **g**, Western blot depicting activation of MPK3 and MPK6 by PrpL or ArgC or TLCK-treated PrpL or TLCK-treated ArgC. The same molecular weight region of the blot is shown as in **b**. **h**, Growth of *X. campestris* strains 8004/*argC* or 8004/vector in 3-week old *Brassica oleracea* (broccoli) leaves. The data represent the mean  $\pm$  s.d.,  $n = 16$  individual seedlings (c), and  $n = 10$  leaves from 5 plants (e, h); \*\*\* $P < 0.001$ , Student’s *t*-test. The experiments in panels **a** and **d** were repeated three times with similar results and the representative images shown were selected from at least three images.

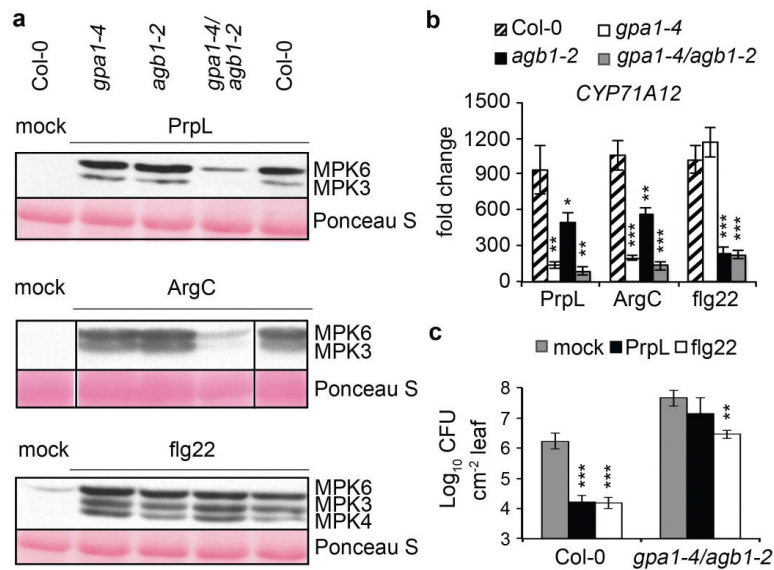


**Figure 2. Protease-mediated defense responses are coupled to G protein signaling**  
**a**, Western blot depicting activation of MAPKs by PrpL, ArgC or flg22 in wild-type Col-0 or G protein T-DNA mutants. The same molecular weight region of the blot is shown as in Fig. 1b. **b**, Induction of defense-related gene expression by PrpL, ArgC or flg22 in wild-type Col-0 or G protein T-DNA mutants measured by RT-qPCR. **c**, Protection of 4-week old wild-type Col-0 or *gab* double mutant leaves from *P. syringae* pv. *tomato* strain DC3000 infection by pre-infiltrated PrpL or flg22. *gpa1-4* is a *ga* mutant; *agb1-2* is a *gb* mutant; and *gpa1-4/agb1-2* is a *gab* double mutant. The data represent the mean  $\pm$  s.d.,  $n = 3$  biological replicates with each experiment containing eight seedlings (**b**), and  $n = 10$  leaves from 5 plants (**c**); \* $P < 0.05$ ; \*\* $P < 0.01$ ; \*\*\* $P < 0.001$ , Student's *t*-test vs. Col-0 (**b**) and vs. mock (**c**).

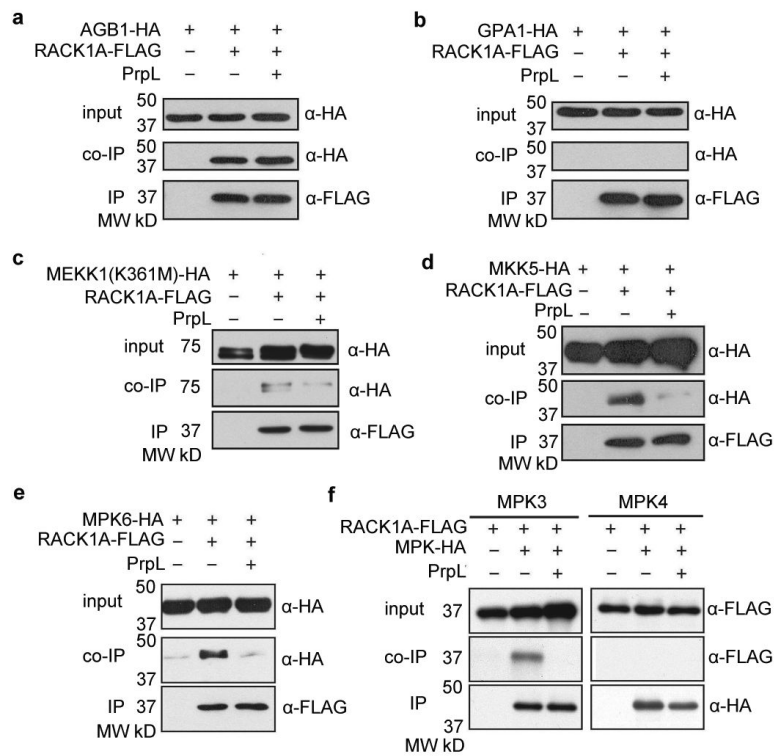


**Figure 3. RACK1A interacts with Gβ and MAPKs**

**a to f**, Co-immunoprecipitation assays in *Arabidopsis* protoplasts. Protoplasts were treated with 100 nM purified PrpL for 15 minutes. Target proteins were detected in Western blots using anti-HA or anti-FLAG antibodies. Numbers left of blots represent marker size in kDa.

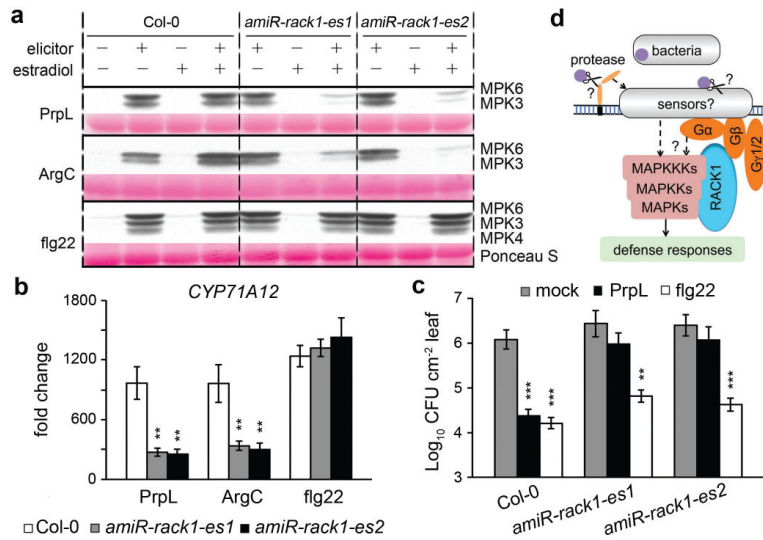


**Figure 4. Transiently silencing all three *rack1* genes abrogates proteases but not flg22-mediated responses**

**a**, Three-day old wild-type Col-0 and transgenic *Arabidopsis* seedlings from two independent *amiR-rack1-es* lines were treated with estradiol to activate expression of the artificial microRNA constructs and then two days later were treated with PrpL, ArgC or flg22 and harvested for the MAPK phosphorylation assay. The same molecular weight region of the Western blot is shown as in Fig. 1b. **b**, Seedlings were treated with estradiol followed by PrpL, ArgC or flg22 as in panel **a** and then harvested for RT-qPCR analysis of *CYP71A12* transcript levels. Water-treated Col-0 was used as a normalization control. **c**, Protection of 4-week old wild-type Col-0 and transgenic *amiR-rack1-es1* or *amiR-rack1-es2* plants from *P. syringae* pv. *tomato* strain DC3000 infection mediated by PrpL or flg22 24 hours after treatment with estradiol. The data represent the mean  $\pm$  s.d.,  $n = 3$  biological replicates with each experiment containing twelve seedlings (**b**), and  $n = 10$  leaves from 5 plants (**c**); \*\* $P < 0.01$ ; \*\*\* $P < 0.001$ , Student's *t*-test vs. Col-0 (**b**) and vs. mock (**c**). **d**. A model of protease-activated novel innate immune signaling pathway in *Arabidopsis*.